

SI Appendix

1. Sources of reagents and preparation of the DNA substrate for observation in solution with magnesium ions

T7 pol, T4 DNA polymerase and KF were purchased from Amersham biosciences (Piscataway, NJ). Sequenase was from USB Corporation (Cleveland, OH). DNA oligomers were custom synthesized by IDT Inc. (Coralville, IA) or MWG-biotech inc. (High Point, NC) followed by additional HPLC or PAGE purification. dNTPs were purchased from Invitrogen (Carlsbad, CA). 2',3'-Dideoxynucleoside triphosphates (ddNTPs) were purchased from Trilink biotechnology (San Diego, CA). Functionalized PEG-NHS and biotin-PEG-NHS were purchased from Nektar Therapeutics (San Carlos, CA).

T7 DNA polymerase requires magnesium ions for its synthesis and editing functions. In order to ensure that the observation of polymerase-dNTP interactions occur at the same template/primer junction, the editing functions that excise nucleotide residues from the primer strand need to be suppressed. For this purpose a modified primer (IDT) with the sequence was used:

Primer: 5' -GCCTCGCAGCCGTCCAACCAACT*C -3' (thioP)

where * denotes the phosphorothioate modification that was introduced to prevent the exonuclease digestion of the primer. The phosphorothioate bond from chemical DNA synthesis has two configurations R_p and S_p for the chiral phosphorus atom. The S_p configuration of the phosphorothioate cannot be digested by the exonuclease activity of polymerases(1). To remove the exonuclease susceptible R_p portion of the primer, 10 μ L 100 μ M thioP primer was incubated with \sim 4 μ M T7 pol for 1 hr in the presence of 10 mM Mg^{2+} . After incubation, the solution was heated to 90 $^{\circ}$ C for \sim 30 min to inactivate the T7 pol. The remaining oligonucleotide was resistant to exonuclease digestion by T7 pol. The DNA duplex Cy3-thioP/T was formed by mixing the Cy3-T oligo and the

selected thioP with a 1/1.5 ratio in phosphate buffer. To form the same sequence as the Cy3T/P duplex, a ddA base was incorporated at the 3' primer terminus by adding into a 10 μ l solution of 4 μ M Cy3-thioP/T duplex with 10 mM MgCl₂, 1 μ l of 10 mM ddATP and 1 μ L of 1 μ M Sequenase solution and incubated for 10 min. The Cy3-ddP/T duplex prepared in this way has the same sequence as the Cy3-P/T, but the ddP primer terminus lacks the 3' -OH group. Thus the primer in the duplex is not extendable. To maintain the ddA base at the 3' end of the primer, 20 μ M ddATP was added to the solution during single molecule observations or for fluorescence titration.

2. Microscope sample preparation and single molecule imaging:

Biotin-functionized glass coverslips were prepared by the following procedure. After thorough cleaning with ethanol and 1 M sodium hydroxide, the No.1 microscope glass slips (VWR Inc., West Chester, PA) were amine-functionalized by treatment with 2% 3-aminopropyl-triethoxysilane in dry acetone for 2 minutes. After rinsing with deionized water, the slips were incubated for 4 hours in a solution of amine-reactive poly(ethylene glycol) (100 mg/ml mPEG-SPA (MW = 5,000) and 1 mg/ml biotin-PEG-CO₂NHS (MW = 3,400) in 100 mM pH 8.3 NaHCO₃).

To immobilize Cy3-P/T duplex, a streptavidin coating was introduced by flowing in 0.2 mg/ml streptavidin (Sigma) and incubated for 10 minutes to provide binding sites for the biotin-modified DNA duplex. After flushing out the excess streptavidin with 3ml phosphate buffer, 10 pM of biotinated Cy3-P/T duplex was introduced and incubated for 10 minutes. Finally the flow cell was flushed with 2 ml of phosphate buffer.

An inverted fluorescence microscope (Olympus IX70, Olympus America Inc., Melville, NY) was used for imaging of the fluorescent DNA duplex attached to the surface of the coverslip. The 532 nm laser (λ -Pro, Shanghai, China) was reflected by a dichroic mirror (Z532, Chroma, Rockingham, VA) and focused onto the edge of the back focal plane of a

microscope objective (60X PlanApo; N.A.=1.45; Olympus) to create a total internal reflection excitation at the interface of glass and water at a power density of $\sim 200\text{W}/\text{cm}^2$. The fluorescence of individual molecules was collected by the same objective and, after passing 3 filters (dichroic mirror Z532, emission filter HQ575/60 and long pass filter 550LP; Chroma, Brattleboro, VT), focused onto a CCD camera (Cascade 512B, Roper Scientific, Trenton, NJ) by the microscope tube lens. Fluorescence movies were recorded at a speed of 5 frames per second. To prevent photobleaching of the fluorescent probe, buffer solutions containing 0.1mg/ml glucose oxidase (Sigma), 0.025mg/ml catalase (Roche), 0.4% (w/v) glucose and 1% beta-mecaptoethanol were used. T7 pol and dNTPs were introduced through the tubing with an automated syringe pump (Harvard Apparatus, PhD 2000, Holliston, MA). Fluorescence intensity time trajectories of individual molecules were extracted from the CCD movie by integrating 2x2 pixels at the fluorescence spot using a Matlab script. The long-term intensity drifts due to objective focus drifts were corrected by dividing a polynomial function that fits the gradual intensity changes in the trajectory. Typically about 50% of the Cy3 labeled DNA molecules were active. We used more than 30 molecules to construct a decay histogram for one experimental condition.

3. Intensity trajectories of various DNA polymerases upon incubation with Cy3-P/T

The binding of DNA polymerases other than T7 pol was also tested. Due to different environments of the Cy3, the binding of various DNA pols have intensity enhancement that are characteristic of the individual DNA pol. Figure S1A shows the fluorescence intensity trajectories of the Cy3-P/T DNA duplex when flowing in T4 pol, KF and sequenase. Binding of the T4 pol and KF leads to enhancement of the Cy3 fluorescence intensity with different amplitudes. However, binding of Sequenase does not change the fluorescence intensity of the Cy3-P/T duplex.

Under the condition where the Cy3 probe is closer to the primer-template junction, we

observed similar Cy3 fluorescence enhancement upon binding of T7 pol and Sequenase to the DNA substrate. Figure S1B shows typical fluorescence intensity trajectories of an immobilized Cy3 labeled DNA duplex, when flowing in 500 nM dNTPs along with T7 pol or Sequenase in Tris buffer with Mg^{2+} . When the 5' overhang of the DNA template was filled by primer extension, binding of Sequenase enhanced the Cy3 fluorescence with an amplitude comparable to that of T7 pol.

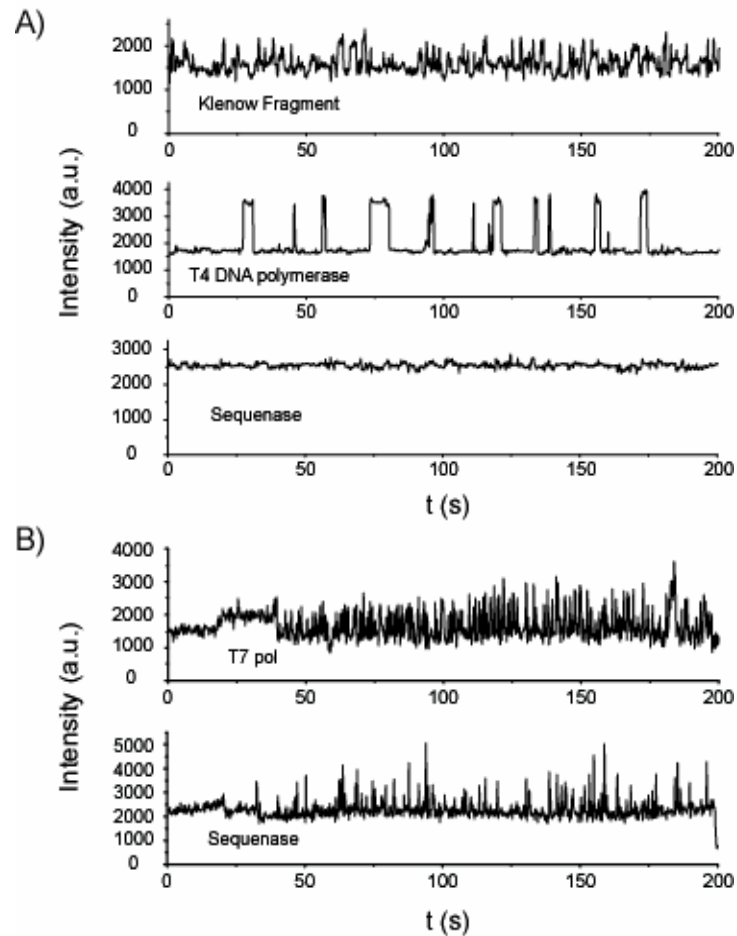


Figure S1 A) Intensity trajectories of the Cy3-P/T DNA duplex in the presence of different DNA polymerases. The binding of KF induced a small but discernable increase of the fluorescence intensity of the Cy3 probe. T4 pol gives a remarkably distinct intensity enhancement. The binding of Sequenase cannot be observed from the fluorescence intensity trajectory. B) Intensity trajectories of individual Cy3 labeled DNA duplex with sequence:

Primer 5' -GCCTCGCAGCCGTCCAACCAACTCC -3' (TP)

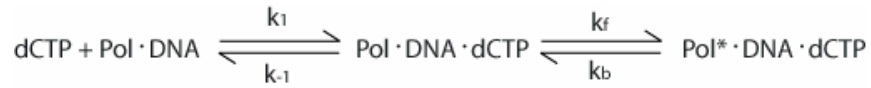
Template 3' -BiotinTEG-CGGAGCGTCGGCAGGTTGGTTGAGGACCTTCTC-Cy3-5' (LCy3T).

Reaction mixture of 500nM dNTPs with T7 pol or Sequenase was flowed in at about 20 second in the trajectory. Different from T7 pol, binding of Sequenase did not result in Cy3 fluorescence changes right after its introduction into the reaction mixture. With the completion of primer extension, the Cy3 moved closer to the polymerase active center; binding of T7 pol and Sequenase yielded similar fluorescence enhancement.

4. Relationship between K_d , K_m and $K_{d,app}$ of dCTP

We noticed that a very low [dCTP] (on the order of 100 nM, much lower than ground state binding constant, which is about 10 μ M, of correct dNTP) could drive the binding to favor the ternary complex. The biased equilibrium of the conformational change after dNTP binding can explain this.

The apparent binding constant $K_{d,app}$ of dCTP from our measurement, defined by the equilibrium constant for the equilibrium between the DNAPol/DNA binary complex and all forms of the DNAPol/DNA/dNTP ternary complex, is different from its K_d and K_m . Consider the following reaction mechanism to clarify their relationship,



where an additional conformational change occurs after dCTP binding. $K_d = \frac{k_{-1}}{k_1}$, is

the binding constant of the initial binding equilibrium. K_m is defined as $K_m = \frac{k_{-1} + k_f}{k_1}$.

Calculation of $K_{d,app}$ needs to take into account all the forms of the ternary complex,

$$K_{d,app} = \frac{[dCTP][Pol \cdot DNA]}{[Pol \cdot DNA \cdot dCTP] + [Pol^* \cdot DNA \cdot dCTP]}.$$

With the relationship $[Pol^* \cdot DNA \cdot dCTP] = \frac{k_f}{k_b} [Pol \cdot DNA \cdot dCTP]$ and

$$[Pol \cdot DNA \cdot dCTP] = \frac{k_1}{k_{-1}} [Pol \cdot DNA][dCTP],$$

we have $K_{d,app} = \frac{k_{-1}}{k_1(1 + k_f/k_b)} = K_d \frac{1}{1 + k_f/k_b}$. In the case of T7 pol, k_f is much larger

than k_b . Finally the relationship $K_{d,app} \approx \frac{k_b}{k_f} K_d \approx \frac{k_b}{k_f} K_m$ explains why we obtained a much lower $K_{d,app}$ of dCTP than the K_d obtained from previous kinetic measurements.

5. Intensity trajectories of T7 pol: Cy3-ddP/T using different concentrations of dCTP with 20 and 100 μM Mg^{2+}

Fluorescence intensity trajectories of the Cy3T/thioPddA duplex with T7 pol and with different concentrations of dCTP in the presence of 20 and 100 μM Mg^{2+} were also recorded. Figure S2A and B are examples of the fluorescence intensity trajectories obtained. The forward and reverse transitions can also be observed at these Mg^{2+} concentrations within the dCTP concentration range used. We observed a higher $K_{d,app}$, compared to values at high (10 mM, where $K_{d,app} \sim 50$ nM) Mg^{2+} concentrations. These observations agree well with the fluorescence intensity titration result.

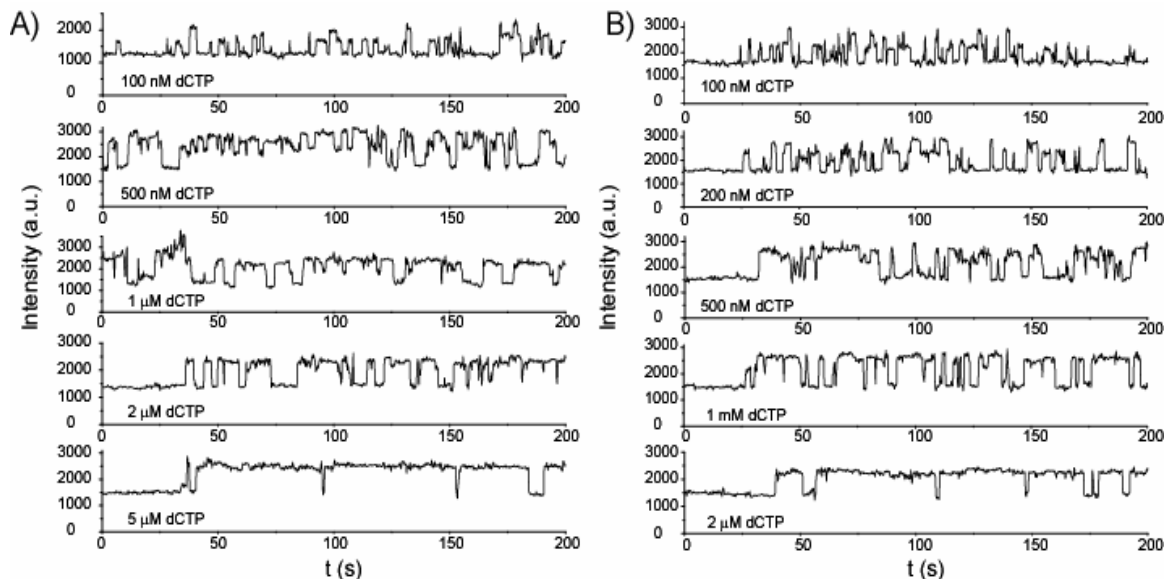


Figure S2 Fluorescence intensity trajectories of the Cy3 probe upon polymerase binding to the P/T in the presence of different concentrations of dCTP in 20 and 100 μM Mg^{2+} . A) With 20 μM magnesium ion, the switching between binary and ternary complexes can be best observed at ~ 500 nM dCTP. B) With 100 μM Mg^{2+} , the switching can be best observed at ~ 200 nM dCTP.

6. Determination of magnesium ion concentrations in phosphate buffer

Calmagite was used to quantify the free Mg^{2+} in the 50 mM pH7.5 phosphate buffer that we used. Shown in Fig. S3A, are a series of absorption spectra of 14 μM calmagite in 250mM pH10 borate buffer with different amounts of added magnesium ion. The absorption spectrum of calmagite in 250 mM pH10 borate solution in the presence of 500 μM EDTA was also measured as a reference for zero magnesium ion concentration. A calibration curve was made by plotting the ratio of the absorbance at 541 and 613 nm from the spectra versus the added magnesium ion concentration (Fig. S3B). By comparing the A_{541}/A_{613} ratio of the absorption spectrum with the calibration curve, we determined that the magnesium ion concentration in 50 mM phosphate buffer was about 3 μM .

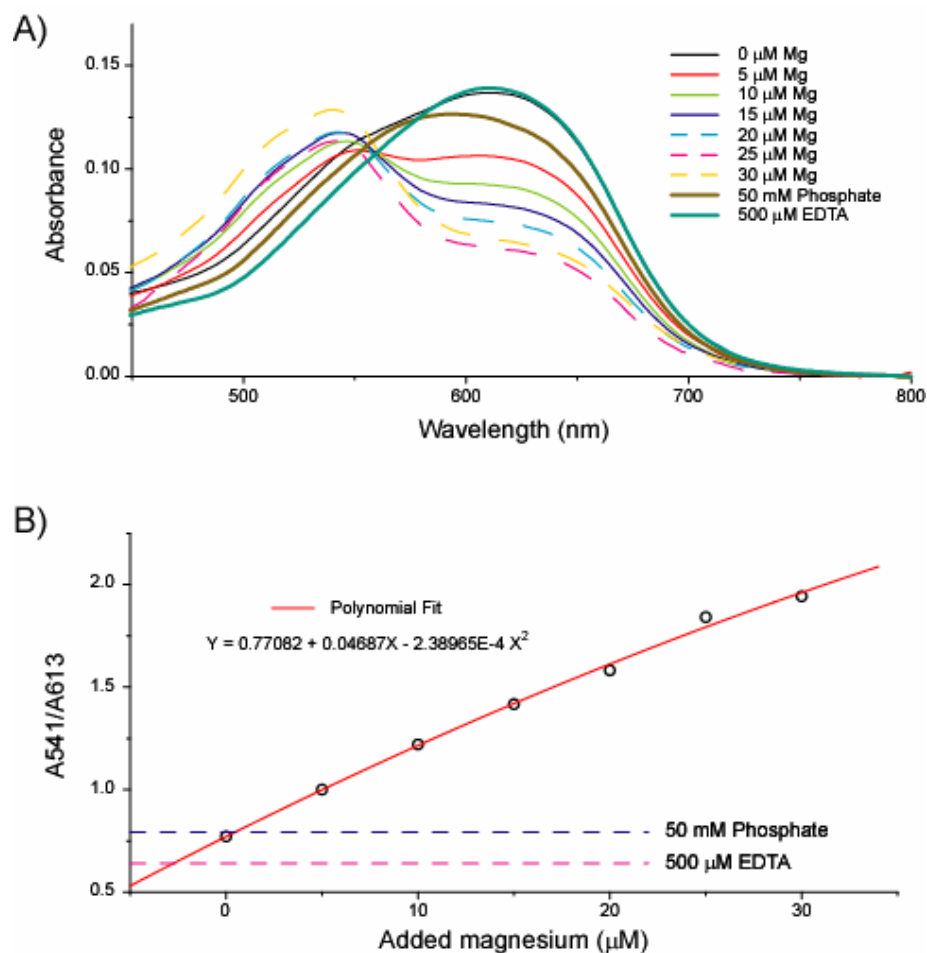


Figure S3 Measurement the magnesium ion concentration in 50 mM phosphate buffer pH7.5. A) Absorption spectra of 14 μM calmagite in different solutions as indicated in the figure. B) Calibration curve for the determination of the magnesium ion concentration in the 50mM phosphate buffer. In the plot, the x-axis is the added amount of magnesium ion in the pH10 borate buffer. A second order polynomial fit was used to model the relationship between the absorbance ratio and the magnesium ion concentration. The blue dashed line shows the absorption ratio of calmagite in the phosphate buffer. As there are still tiny amounts of magnesium ions in the borate buffer, absorption spectrum of calmagite in the solution containing 500 μM EDTA was used as a reference for the absorption ratio without magnesium (red dashed line).

7. Intensity trajectories of duplex Cy3-P/T with T7 pol and dCTP in 50 mM phosphate buffer containing 3 μM Mg^{2+} .

We noticed that the binding of dCTP still induced similar conformational changes in the polymerase complex as observed in the fluorescence trajectories of Cy3-P/T in the phosphate buffer without EDTA. Fig. S4 shows examples of the fluorescence trajectories obtained with the Cy3-P/T duplex in a solution of 5nM T7 pol and different concentrations of dCTP. Repetitive binding events with the identical single DNA duplex can be observed. The $K_{d,app}$ of dCTP under these conditions is much greater than at high Mg^{2+} concentration. In the dCTP concentration range of 1~10 μ M, conformational changes of the polymerase can be observed from the fluorescence intensity trajectories. In the phosphate buffer, the non-complementary substrate, dGTP, at a concentration of 250 μ M did not change the binding pattern of the trajectory (data not shown).

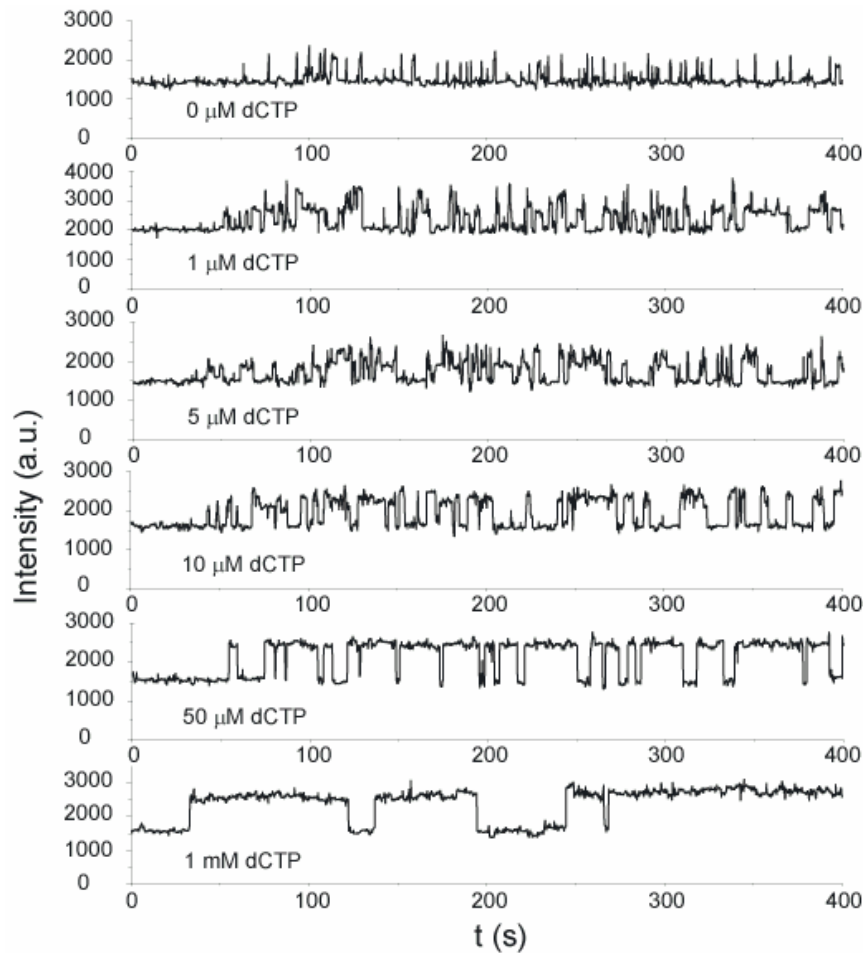
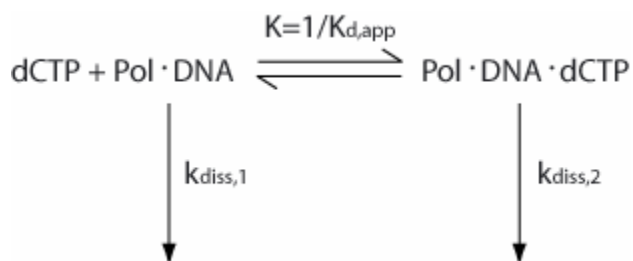


Figure S4 Fluorescence intensity trajectories of the Cy3-P/T duplex with 5nM T7 pol and different concentrations of dCTP in 50 mM phosphate buffer (with $\sim 3 \mu\text{M}$ of Mg^{2+}).

8. dCTP concentration dependence of the polymerase:DNA dissociation rate

We observed that the binding of the dCTP substrate to the polymerase/DNA complex changed the dissociation rate of the polymerase from the DNA. This observation can be explained by the following scheme,



in which the polymerase dissociation from DNA can occur from both the binary and ternary complex. The dCTP concentration affects the equilibrium between the binary and ternary complexes with an apparent binding constant $K_{d,app}$. The binding and dissociation of dCTP from T7 pol complexes is faster than the polymerase dissociation rate from its DNA complexes. The average dissociation rate then is determined by the population of the polymerase in binary and ternary complexes p_{bin} and p_{ter} ,

$$k_{diss} = k_{diss,1} p_{bin} + k_{diss,2} p_{ter}.$$

With the relation $p_{bin} = \frac{K_{d,app}}{K_{d,app} + [dCTP]}$ and $p_{ter} = \frac{[dCTP]}{K_{d,app} + [dCTP]}$,

the dCTP concentration dependent average dissociate rate of the polymerase is

$$k_{diss} = k_{diss,1} \frac{K_{d,app}}{K_{d,app} + [dCTP]} + k_{diss,2} \frac{[dCTP]}{K_{d,app} + [dCTP]}$$

The amplitude of the change in k_{diss} at different dCTP concentrations depends on the difference of $k_{diss,1}$ and $k_{diss,2}$. The change of k_{diss} of DNA pol from Cy3-ddP/T upon dCTP binding with 10mM Mg^{2+} is noticeable. In phosphate buffer the k_{diss} changes by over 10 fold with the addition of dCTP. The reduced dissociation rate can be rationalized in terms of the structure of the T7 pol ternary complex, where the fingers domain is in the closed position, restricting the motion of the P/T. Shown in Fig. S5 is the [dCTP] dependence of k_{diss} in phosphate buffer. Also shown is the curve used to fit the model presented above. The $K_{d,app}$ of dCTP is 6 μ M under these conditions.

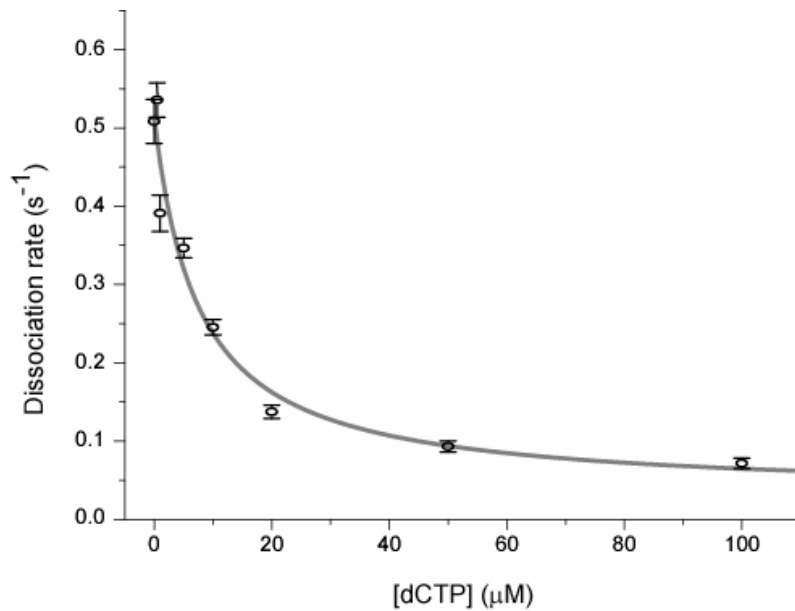


Figure S5 dCTP concentration dependence of the polymerase dissociation rate obtained from the statistics of the binding durations at different dCTP concentrations. A fit

$$k_{diss} = k_{diss,1} \frac{K_{d,app}}{K_{d,app} + c} + k_{diss,2} \frac{c}{K_{d,app} + c}$$

was used to model the data. An apparent dCTP binding

constant $K_{d,app}$ of $\sim 6 \mu$ M was obtained.

9. Incorporation test using phosphate buffer

Fluorescence resonance energy transfer (FRET) between Cy3 and Dabcyl was used to

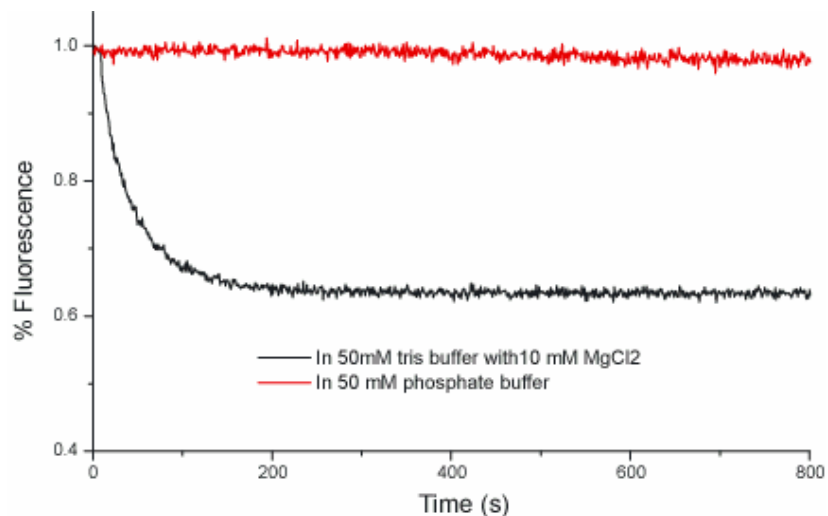
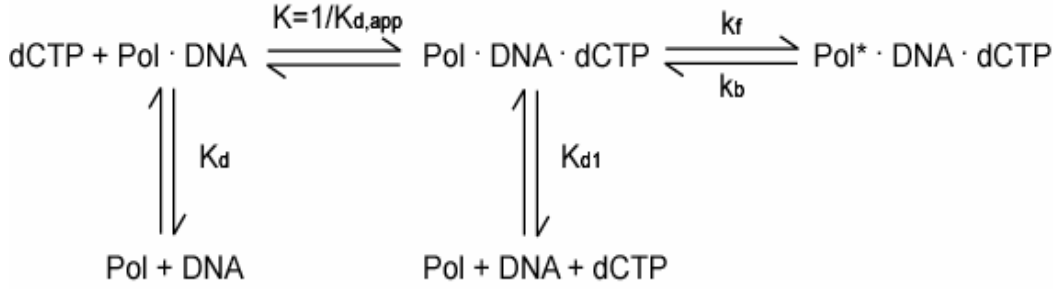


Figure S6 Fluorescence intensity of the Cy3 probe in the LCy3T/TP DNA duplex in the presence of 400 nM Dabcyl-dUTP and 1.4 nM sequenase in different reaction buffers. Clearly, at a magnesium concentration of 3 μM , the incorporation reaction catalyzed by Sequenase is negligible during this period.

10. Determination of $K_{d,app}$ using fluorescence intensity titration

To explore the effect of $[\text{Mg}^{2+}]$ on the rate of conformational change, the change of fluorescence intensity of the T7 pol: Cy3-ddP/T complex upon addition of dCTP, at the ensemble-averaged level, were used to determine the $K_{d,app}$ of dCTP at different $[\text{Mg}^{2+}]$. In the fluorescence intensity titrations, different $[\text{Mg}^{2+}]$ were employed and measurements were made using a spectrofluorometer (Fluorolog III, Jobin Yvon Inc.). Solutions of 5nM DNA duplex (Cy3-ddP/T), 13nM T7 pol, 20 μM ddATP, and various $[\text{Mg}^{2+}]$ in 50mM pH7.5 phosphate buffer were titrated with increasing amounts of dCTP. The fluorescence intensities of the Cy3 probe (excited at 532nm and emission at 563nm) were recorded at each [dCTP].

It is convenient to determine the apparent binding constant of dCTP using the fluorescence intensity titration. Consider the equilibrium as follows,



Since the polymerase is in excess relative to the DNA duplex, the free polymerase concentration can be treated as constant. There are four different states of the Cy3 probes, (i) in the free DNA duplex; (ii) in the polymerase/DNA binary complex; (iii) in the ternary complex before conformational change; and (iv) in the ternary complex after the conformational change. The total fluorescence intensity is the sum of the intensities of Cy3 probe in different states. Therefore we have

$$I = p_{dna} I_{dna} + p_{pol-dna} I_{pol-dna} + p_{pol-dna-dCTP} I_{pol-dna-dCTP} + p_{pol^*-dna-dCTP} I_{pol^*-dna-dCTP}$$

where p refers to the population and I refers to the intensity. We can simplify this expression by combining the two ternary complex terms into one, as the equilibrium between them is not controlled by the dCTP concentration. In this case the equilibrium constant of the binary complex and ternary complex becomes $K_{d,app}$.

$$I = p_{dna} I_{dna} + p_{pol-dna} I_{pol-dna} + p'_{pol-dna-dCTP} I_{pol-dna-dCTP}$$

With the equilibrium relations we have

$$p_{dna} = \frac{K_{d,pol} K_{d,app}}{K_{d,pol} K_{d,app} + [Pol] K_{d,app} + [Pol][dCTP]} \quad ,$$

$$p_{pol-dna} = \frac{[Pol] K_{d,app}}{K_{d,pol} K_{d,app} + [Pol] K_{d,app} + [Pol][dCTP]} \quad \text{and}$$

$$P'_{pol-dna-dCTP} = \frac{[Pol][dCTP]}{K_{d,pol}K_{d,app} + [Pol]K_{d,app} + [Pol][dCTP]}$$

The total fluorescence intensity is

$$I = \frac{(I_{dna}K_{d,pol} + I_{pol-dna}[Pol])K_{d,app} + I'_{pol-dna-dCTP}[Pol][dCTP]}{(K_{d,pol} + [Pol])K_{d,app} + [Pol][dCTP]}$$

In our titration experiments, $[Pol]$ is about 10 nM and the $K_{d,pol}$ is about 20 nM. With these parameters fixed, we can determine the $K_{d,app}$ with the fluorescence titration.

Figure S7A shows an example of the fluorescence intensity as a function of $[dCTP]$ in the presence of 100 μM MgCl_2 . The $K_{d,app}$ for dCTP binding decreases with increasing $[\text{Mg}^{2+}]$ as shown in Fig. S7B. This result is in good agreement with the single-molecule observations, namely that Mg^{2+} facilitates the forward conformational change but has little effect on its reversal. The effect of $[\text{Mg}^{2+}]$ on dCTP binding at the ensemble averaged level saturates in the mM range.

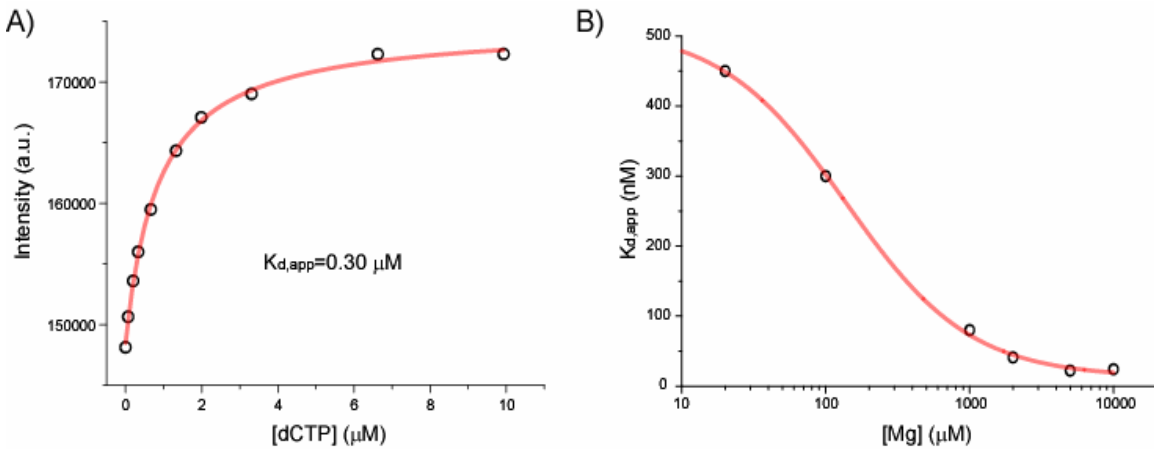


Figure S7 A) An example of fluorescence intensity titration to determine the apparent binding constant $K_{d,app}$ of dCTP to the T7 pol/DNA binary complex in the presence of 100 μM Mg^{2+} . A fit

$$I = \frac{(I_{dna}K_{d,pol} + I_{pol-dna}[Pol])K_{d,app} + I'_{pol-dna-dCTP}[Pol][dCTP]}{(K_{d,pol} + [Pol])K_{d,app} + [Pol][dCTP]}$$

determined to be 0.30 μM . **B**) $[\text{Mg}^{2+}]$ dependence of the $K_{d,app}$ of dCTP binding. At each $[\text{Mg}^{2+}]$, the $K_{d,app}$ of dCTP was determined by fluorescence intensity titrations. The relation

$$K_{d,app} \approx K_m \frac{1 + [\text{Mg}^{2+}] / K_{d,Mg}}{k_{f1} / k_{b1} + (k_{f2} / k_{b2}) [\text{Mg}^{2+}] / K_{d,Mg}}$$

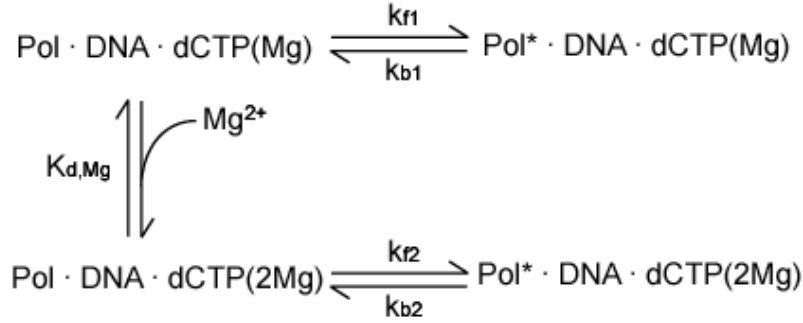
$K_{d,app}$. The binding affinity of magnesium $K_{d,Mg} = 5 \text{ mM}$ was obtained from the curve fitting.

11. The $K_{d,app}$ for dCTP binding depends on $[\text{Mg}^{2+}]$

At very low $[\text{Mg}^{2+}]$ these conformational changes still occur in the complex between T7 pol and DNA duplex Cy3-P/T with the extendable primer P, even in the absence of chemistry. The K_d of Mg^{2+} in the B site is much lower than the K_d for Mg^{2+} in the A site. In this case the catalytic A site (see in Fig. 1B in the main text) must be empty, otherwise phosphoryl transfer would occur. This is consistent with the results of the Tsai group on pol β , namely that one metal ion (in the B site) is required to trigger the conformational change(2, 3).

The dependence of the $K_{d,app}$ of dCTP binding on $[\text{Mg}^{2+}]$ can be modeled using a scheme where the polymerase would have different rates of conformational change with different extents of Mg^{2+} occupancy. As the binding of the Mg^{2+} at the B site is relatively tight ($K_d \sim 10 \mu\text{M}$), in the Mg^{2+} concentration range of 20 μM to 10 mM, the first magnesium-binding site B has been saturated. Therefore the $[\text{Mg}^{2+}]$ dependence of dCTP binding for T7 pol is due to the second magnesium ion binding to the catalytic site (A site). Such dependence of the rate on the second Mg^{2+} occupancy (in the A site) is consistent with the assignment of the observed conformational change to polymerase fingers closing, as the second Mg^{2+} will further stabilize the closed conformation.

Our observations can be explained with the parallel kinetic scheme,



We assume the magnesium ion doesn't affect the initial binding equilibrium of the dCTP to the polymerase open complex. From the derivation of the relation of $K_{d,app}$ and K_d , the apparent binding constant of dCTP can be calculated by

$$K_{d,app} \approx K_d \frac{[\text{Pol} \cdot \text{DNA} \cdot \text{dCTP}(\text{Mg})] + [\text{Pol} \cdot \text{DNA} \cdot \text{dCTP}(\text{Mg}_2)]}{[\text{Pol}^* \cdot \text{DNA} \cdot \text{dCTP}(\text{Mg})] + [\text{Pol}^* \cdot \text{DNA} \cdot \text{dCTP}(\text{Mg}_2)]}$$

With the relations of $[\text{Pol}^* \cdot \text{DNA} \cdot \text{dCTP}(\text{Mg})] = \frac{k_{f1}}{k_{b1}} [\text{Pol} \cdot \text{DNA} \cdot \text{dCTP}(\text{Mg})]$,

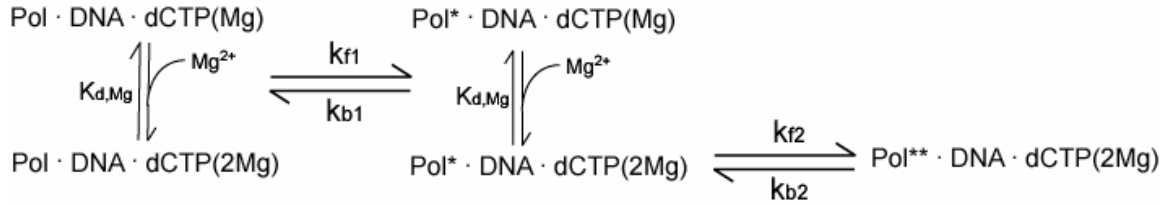
$[\text{Pol}^* \cdot \text{DNA} \cdot \text{dCTP}(\text{Mg}_2)] = \frac{k_{f2}}{k_{b2}} [\text{Pol} \cdot \text{DNA} \cdot \text{dCTP}(\text{Mg}_2)]$, and

$[\text{Pol} \cdot \text{DNA} \cdot \text{dCTP}(\text{Mg}_2)] = \frac{[\text{Mg}^{2+}][\text{Pol} \cdot \text{DNA} \cdot \text{dCTP}(\text{Mg})]}{K_{d,\text{Mg}}}$, we have the expression of

the apparent binding constant $K_{d,app} \approx K_d \frac{1 + [\text{Mg}^{2+}] / K_{d,\text{Mg}}}{k_{f1} / k_{b1} + (k_{f2} / k_{b2}) [\text{Mg}^{2+}] / K_{d,\text{Mg}}}$. A K_d of

5mM for Mg^{2+} occupancy was obtained from curve fitting (Fig. S7B). This value is similar to that reported for the K_d of Mg^{2+} binding to the (catalytic) A site(3).

However, an alternative sequential kinetics scheme shown below can also explain our data.



Here Pol^* and Pol^{**} denote the closed form of T7 pol with one or two Mg^{2+} coordination complexes formed.

From the derivation of the relation of $K_{d,app}$ and K_d , the apparent binding constant of dCTP $K_{d,app}$ can be calculated by

$$K_{d,app} \approx K_d \frac{[\text{Pol} \cdot \text{DNA} \cdot \text{dCTP}]}{[\text{Pol}^* \cdot \text{DNA} \cdot \text{dCTP}] + [\text{Pol}^{**} \cdot \text{DNA} \cdot \text{dCTP}(\text{Mg}_2)]}$$

Finally we have $K_{d,app} \approx K_d \frac{1 + [\text{Mg}^{2+}] / K_{d,\text{Mg}}}{k_{f1} / k_{b1} + k_{f1} / k_{b1} \cdot (1 + k_{f1} / k_{b1}) \cdot [\text{Mg}^{2+}] / K_{d,\text{Mg}}}$. This

expression is equivalent to that from the previous kinetic scheme. Therefore, the same value of $K_{d,\text{Mg}}$ can still be obtained from the $[\text{Mg}^{2+}]$ dependence of the $K_{d,app}$ of dCTP. The major difference between these two kinetic schemes is whether the two Mg^{2+} complexes can be formed in one step. With the current data, we cannot discriminate between them.

12. Experimental result using a different duplex and the complimentary dTTP

The DNA duplex with sequence

Primer: 5' -GCCTCGCAGCCGTCCAACCAACTCC -3' (TP)

Template: 3' -BiotinTEG-CGGAGCGTCGGCAGGTTGGTTGAGGACCTTCTC-Cy3-5' (LCy3T)

was also tested for binding of T7 pol and dTTP. Figure S8A shows examples of the

fluorescence trajectories in the solution of 5nM T7 pol and different concentrations of dTTP in the phosphate buffer. Repeated binding events at the same single DNA duplex can be observed. Similar to the situation when using the duplex Cy3-P/T, longer binding durations and a second intensity level appeared with the addition of dTTP. The dTTP concentration dependence of the polymerase dissociation rate is shown in figure S8B.

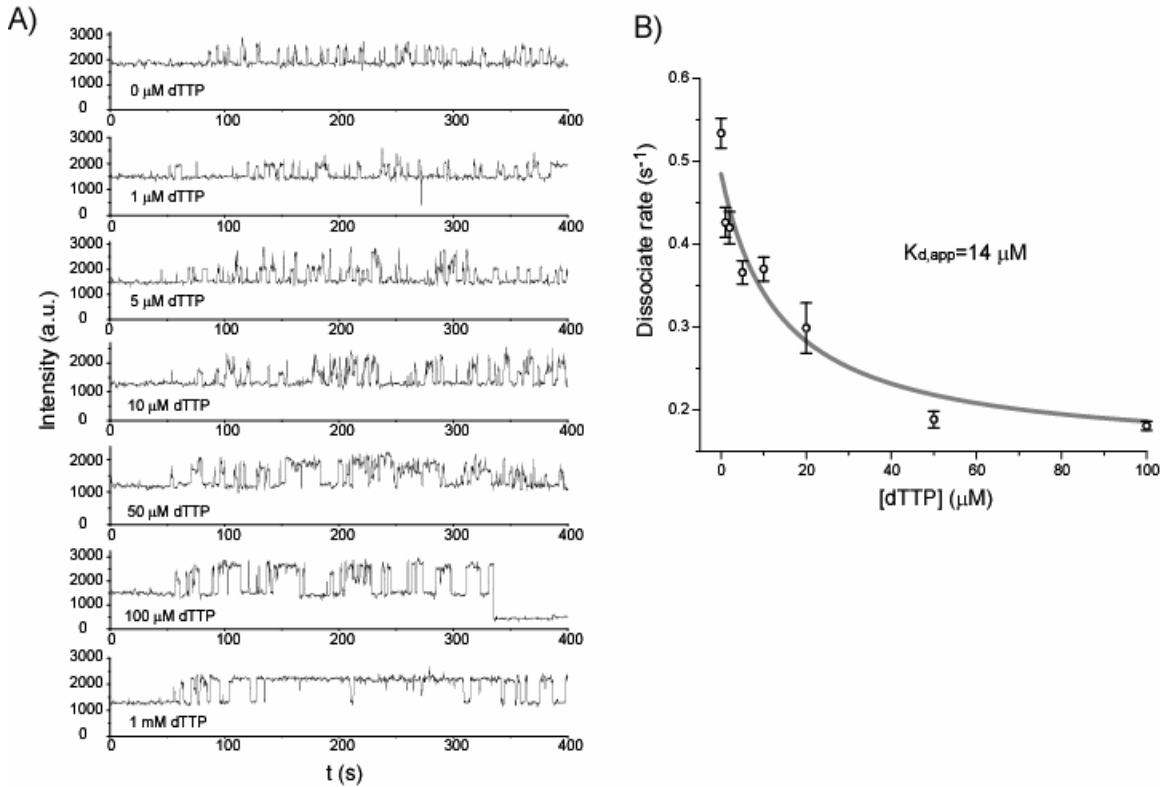


Figure S8 Experimental result with T7 pol and the DNA duplex LCy3T/TP duplex and dTTP. A) Fluorescence intensity trajectory of the Cy3 probe upon polymerase binding to DNA in the presence of different dTTP concentrations in 50 mM phosphate buffer (with ~3 μM magnesium ion). Elongated polymerase binding duration at high dTTP concentration, and transition between polymerase binary and ternary complexes can be observed from these trajectories. B) dTTP concentration dependence of the polymerase dissociation rate. A fit $k_{diss} = k_{diss,1} \frac{K_{d,app}}{K_{d,app} + [dTTP]} + k_{diss,2} \frac{[dCTP]}{K_{d,app} + [dTTP]}$ is used to model the data. The apparent binding constant of dTTP in this case is ~14 μM.

13. Stopped-flow fluorescence measurements

Stopped-flow fluorescence measurements were carried out with an Applied Photophysics SX.18MV stopped-flow spectrofluorometer at 22°C. The instrument triggered a rapid mixing of solutions from two different syringes. One syringe contained 50 nM Cy3-ddP/T duplex, 200 nM T7 pol and 10 μM ddATP in 40 mM pH 7.5 Tris buffer with 10mM MgCl₂. The other syringe was filled with different concentrations of dCTP in 40 mM Tris buffer pH 7.5 containing 10mM MgCl₂. After excitation at 546 nm with a mercury lamp, the fluorescence of the Cy3-ddP/T was detected by a PMT after passing through a 570BP filter and recorded as a function of time. The fluorescence signal was collected for 1s. Two to four traces were averaged for each set of conditions. The dead time of the instrument is 2 ms.

14. Continuous-flow fluorescence measurements using a hydrodynamic focusing device

Since the conformational change of T7 pol: Cy3-T/P: dCTP ternary complex is too fast to be resolved with our stopped-flow instrument, we constructed a microfluidic continuous-flow device based on hydrodynamics focusing according to the report by Knight et al.(4) to make the kinetic measurements. Soft lithography technique was used for the fabrication of this device. Fig. S9 shows the setup for continuous-flow fluorescence measurements.

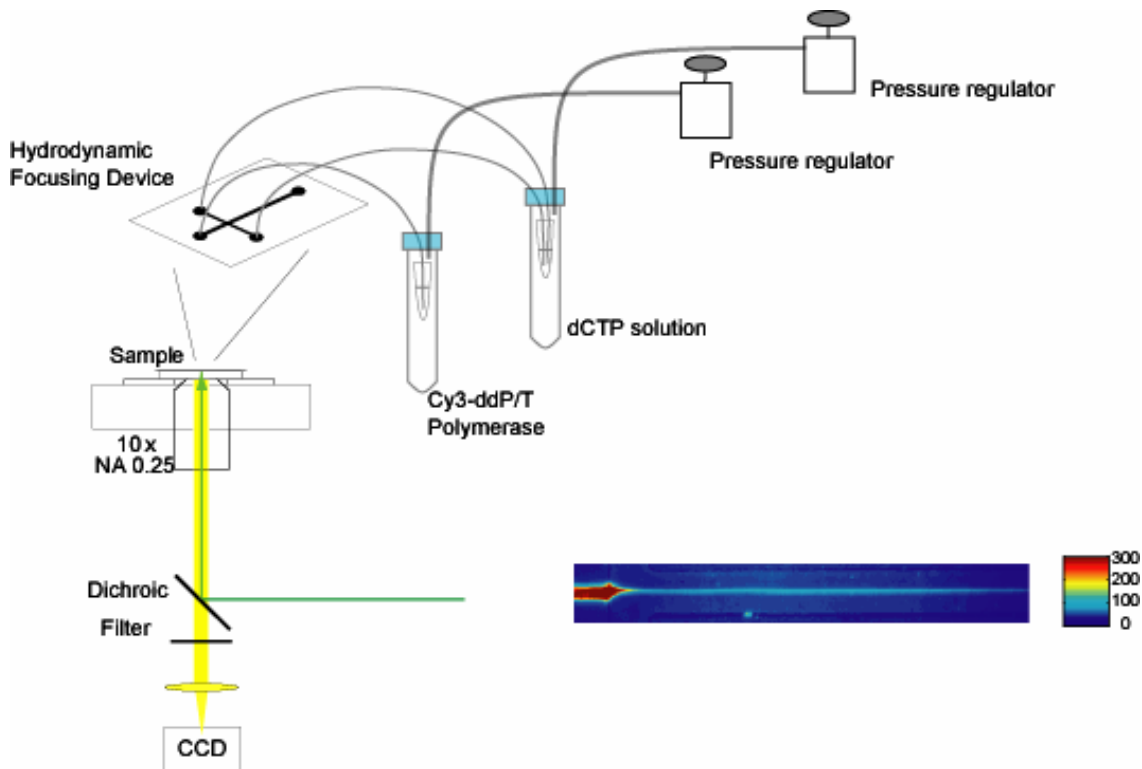


Fig S9 Setup for the continuous-flow fluorescence measurement using hydrodynamics focusing to measure the fast conformational change of the T7 pol ternary complex upon dCTP binding. Hydrodynamic focusing can be realized by applying appropriate pressures to the central and side stream inlets of the microfluidic device. The depths of the microfluidic channels are 20 μm . The width of the central inlet channel, two side channels and focused channel are 10, 40, 40 μm , respectively. To illuminate a large enough area, an Olympus 10x NA 0.25 objective was used to image the flow, the final magnification of the system is 15x. Under these conditions one pixel corresponds to 1.067 μm . The inset in the lower right corner is a typical fluorescence image of the focused stream.

Fast mixing is realized by focusing the central stream into a very narrow range, so that solute in the side streams can diffuse into the central stream within a short time. The width of the focused stream can be controlled by the pressure ratio of the central and side channel inlets. A typical pressure of 6.0 psi for the side and 5.8 psi for the central stream was used, leading to a volume flow rate of 2.5 $\mu\text{l}/\text{min}$, corresponding to a line speed of ~ 75 $\mu\text{m}/\text{ms}$ at the center of the channel. The width of the stream in this condition is ~ 300

nm, measured by the Cy3 fluorescence intensity ratio between the focused area and the pre-focusing area. The estimated mixing time at this stream width is about 50 μ s for the dCTP substrate.

In our experiment the central stream is a pH 7.5 50mM Tris Buffer with 10mM Mg^{2+} , 100nM Cy3-P/ddT and 1 μ M T7 DNA polymerase, and the side stream is a pH 7.5 50mM Tris Buffer with 10mM Mg^{2+} and different concentrations of dCTP. The kinetic information can be obtained by measurement of the fluorescent intensity profile at different positions of the focused stream, translated into different time points after mixing. 500 frames of the fluorescent images were collected, and averaged to obtain an averaged fluorescence image of the focused stream.

The fluorescence intensities at different time were obtained by fitting the line profile in the image across the stream with a Gaussian function. To correct for the uneven illumination of the sample, the intensity profile is normalized by dividing the intensity trace of a control image, which was obtained when a buffer solution without dCTP was supplied in the side channels.

Fig. S10 shows the normalized fluorescence time traces of the Cy3-ddP/T: T7 pol complex when mixing with different concentrations of dCTP.

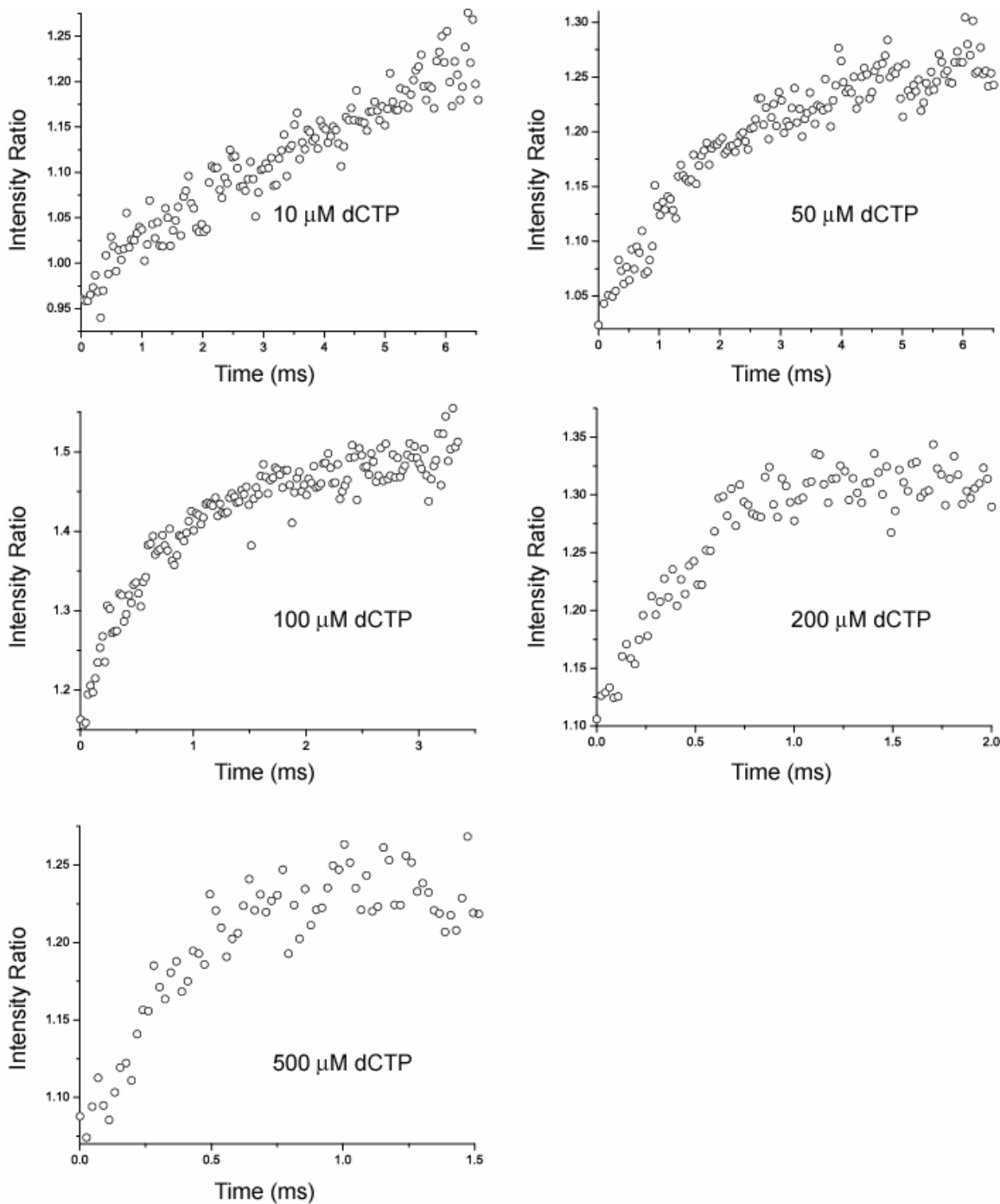


Fig. S10 Normalized fluorescence intensity trace of Cy3-ddP/T: T7 pol complex after mixing with different concentrations of dCTP solution. For 10 and 50 μM dCTP, the line speed of the central stream was $75 \mu\text{m}\cdot\text{ms}^{-1}$. For dCTP concentrations of 100, 200, 500 μM , a higher line speed of the central stream at $150 \mu\text{m}\cdot\text{ms}^{-1}$ was used to increase the time resolution. The relative amplitude of the intensity change is about

25%, matching the expected value. The rate constants for the fluorescence increase were obtained by fitting the traces with a single exponential rise function. At 10 μM dCTP, the rate constant obtained by this method (220 s^{-1}) is consistent with the value obtained from stopped-flow fluorescence measurements.

15. Observation of the conformational change induced by ddCTP binding

The structure of the closed form of T7 pol replication complex was obtained using 3'-dideoxy terminated primer and a dideoxy nucleotide triphosphate ddNTP as the incoming substrate. We also made observation using the Cy3-ddP/T: T7 pol complex and the ddCTP to better connect the fluorescence observation and the previous structural information. A similar fluorescence increase of the Cy3 probe can also be observed upon ddCTP binding, as shown in Fig. S11. The affinity of ddCTP to the T7 pol complex is found to be only slightly lower than that of dCTP. With this observation, we can make a direct connection between this Cy3 fluorescence intensity increase to the fingers closing found by X-ray crystallography.

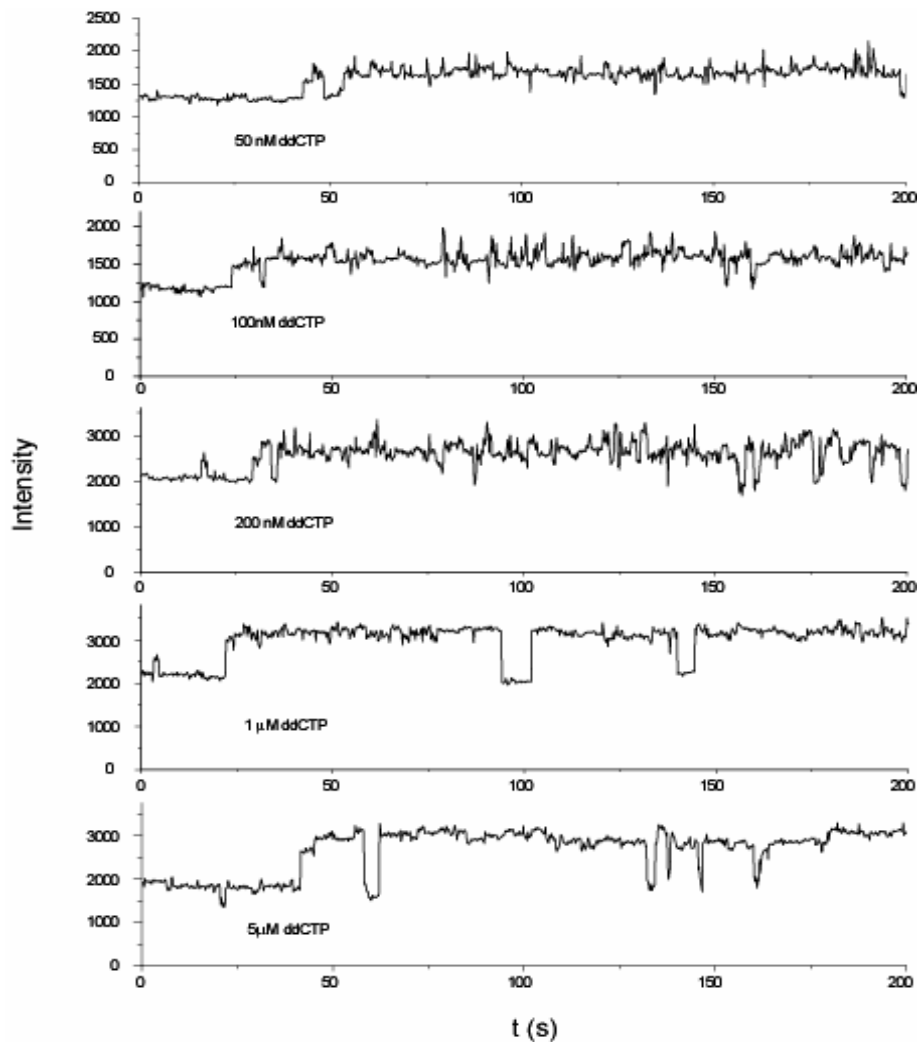


Fig. S11 Fluorescence intensity trajectories of the Cy3-ddP/T upon polymerase binding in the presence of different concentrations of ddCTP. Similar fluorescence intensity enhancement after ddCTP binding to that shown in Fig. 4A in the main text can be observed. The apparent binding constant of ddCTP is on the range of sub-micromolar concentration.

References:

1. Brautigam, C. A. & Steitz, T. A. (1998) *Journal of Molecular Biology* **277**:363-377.
2. Dunlap, C. A. & Tsai, M.-D. (2002) *Biochemistry* **41**:11226-11235.
3. Bakhtina, M., Lee, S., Wang, Y., Dunlap, C., Lamarche, B. & Tsai, M.-D. (2005)

Biochemistry **44**:5177-5187.

4. Knight, J. B., Vishwanath, A., Brody, J. P. and Austin, R. H. (1998) *Phys. Rev. Lett.* **80**: 3863-3866.